ADAM9 enhances Th17 cell differentiation and autoimmunity by activating TGF-β1

Masataka Umeda[a,1], Nobuya Yoshida[a,1], Ryo Hisada[a], Catalina Burbano[a], Seo Yeon K. Orite[a], Michihito Kono[a], Vasileios C. Kyttaris[a], Suzanne Krishfield[a], Caroline A. Owen[b], and George C. Tsokos[a,2]

[a]Department of Medicine, Beth Israel Deaconess Medical Center, Harvard Medical School, Boston, MA 02215; and [b]Division of Pulmonary and Critical Care Medicine, Brigham and Women's Hospital, Harvard Medical School, Boston, MA 02115

Edited by Marc K. Jenkins, University of Minnesota Medical School, Minneapolis, MN, and approved March 30, 2021 (received for review November 9, 2020)

The a disintegrin and metalloproteinase (ADAM) family of proteinases alter the extracellular environment and are involved in the development of T cells and autoimmunity. The role of ADAM family members in Th17 cell differentiation is unknown. We identified ADAM9 to be specifically expressed and to promote Th17 differentiation. Mechanistically, we found that ADAM9 cleaved the latency-associated peptide to produce bioactive transforming growth factor β1, which promoted SMAD2/3 phosphorylation and activation. A transcription factor inducible cAMP early repressor was found to bind directly to the *ADAM9* promoter and to promote its transcription. *Adam9*-deficient mice displayed mitigated experimental autoimmune encephalomyelitis, and transfer of *Adam9*-deficient myelin oligodendrocyte globulin-specific T cells into *Rag1*$^{-/-}$ mice failed to induce disease. At the translational level, an increased abundance of ADAM9 levels was observed in CD4$^+$ T cells from patients with systemic lupus erythematosus, and ADAM9 gene deletion in lupus primary CD4$^+$ T cells clearly attenuated their ability to differentiate into Th17 cells. These findings revealed that ADAM9 as a proteinase provides Th17 cells with an ability to activate transforming growth factor β1 and accelerates its differentiation, resulting in aberrant autoimmunity.

a disintegrin and metalloproteinase | systemic lupus erythematosus | Th17 cell

Systemic lupus erythematosus (SLE) afflicts more than a million Americans—the majority of whom are women—and the disease is more severe among minorities. The disease is clinically heterogenous with manifestations from every organ, while numerous mechanistic pathways have been identified to propagate an autoimmune response leading to inflammation in multiple organs (1). Among the cellular abnormalities, T cells contribute in important ways by providing help to B cells and producing inflammatory cytokines including interleukin-17 (IL-17) (2). IL-17 induces the production of additional inflammatory cytokines and chemokines, which engage monocytes and neutrophils in the expression of inflammation (3, 4). Patients with SLE have an increased number of Th17 cells both in the peripheral blood and in inflamed tissues, including the kidneys (5, 6).

Th17 cell differentiation is regulated by proinflammatory cytokines including transforming growth factor-β1 (TGF-β1) and IL-6 (7). Metalloproteinases act as sheddases to alter extracellular and cell surface molecules including cytokines, chemokines, and receptors that are involved in T cell differentiation (8). It is noteworthy that a disintegrin and metalloproteinases (ADAMs), a family of transmembrane proteins with disintegrin and metalloproteinase domains, are important in the regulation of T cell function by cleaving enzymatically key factors in various immune responses (9). For example, both ADAM10 and ADAM17 cleave IL-6 receptor (IL-6R), and the cleaved soluble-IL-6R activates T cells through gp130 irrespective of whether the cells express IL-6R (10). In addition, ADAM10 cleaves IL-2Rβ from the cell surface of regulatory T (Treg) cells and mitigates its signaling capacity (11). In SLE, ADAM10 is known to have a pivotal role in the development of aberrant autoimmunity by cleaving Axl, a transmembrane activator and CAML interactor, and fractalkine (12–14).

ADAM9 is a type I transmembrane protein containing a metalloproteinase domain responsible for proteolysis with 82% identity between mice and humans (15). It has been implicated in retinal neovascularization (16, 17) and tumor progression (18–20). Several immune cells express ADAM9 including monocytes (21), macrophages (22), and polymorphonuclear neutrophils (23). The list of potential ADAM9 substrates linked with the immune system is expanding and includes epidermal growth factor, vascular cell adhesion protein, VE-cadherin, CD40, fibroblast growth factor receptor-2IIIb, and vascular endothelial growth factor receptor 2 (17, 20). Yet it is not known whether ADAM9 is involved in any T cell function.

In this study, we reveal that ADAM9 is specifically expressed in Th17 cells and promotes their differentiation by activating TGF-β1 and promoting SMAD2/3 phosphorylation. The transcription factor inducible cAMP early repressor (ICER) accumulates on the *ADAM9* promoter and promotes ADAM9 gene transcription. *Adam9*-deficient mice developed less experimental autoimmune encephalomyelitis (EAE), whereas CD4$^+$ T cells from SLE patients displayed increased expression of ADAM9, and deletion of *ADAM9* attenuated their ability to differentiate to Th17. Collectively, our results show that ADAM9 is pivotal for the differentiation of Th17 cells and that it can be targeted for therapeutic purposes in diseases that depend on Th17-mediated immunopathology.

Significance

Members of the ADAM family of proteinases are expressed by immune cells and have been postulated to contribute to the development of autoimmune pathology. The current report provides evidence that ADAM9 drives the development of Th17 cells by producing bioactive TGF-β1. ADAM9 deficiency mitigates experimental autoimmune encephalomyelitis in mice, while T cells from patients with systemic lupus erythematosus express increased amounts of ADAM9, which, when suppressed, mitigates the generation of Th17 cells. The findings of this study identify the pivotal role of ADAM9 in the development of Th17 cells, and its targeting should ameliorate pathology in Th17-dependent diseases.

Author contributions: M.U., N.Y., and G.C.T. designed research; M.U., N.Y., R.H., C.B., S.Y.K.O., M.K., V.C.K., S.K., and C.A.O. performed research; M.U. and N.Y. analyzed data; and M.U., N.Y., and G.C.T. wrote the paper.

The authors declare no competing interest.

This article is a PNAS Direct Submission.

[1]M.U. and N.Y. contributed equally to this work.

[2]To whom correspondence may be addressed. Email: gtsokos@bidmc.harvard.edu.

This article contains supporting information online at https://www.pnas.org/lookup/suppl/doi:10.1073/pnas.2023230118/-/DCSupplemental.

Published April 28, 2021.

Results

ADAM9 Is Expressed Exclusively in Th17 Cells and Promotes Their Differentiation. To assess the expression pattern of members of the ADAM family in Th17 cells, we first assessed mRNA-encoding ADAM family member expression in murine T cells cultured in vitro under Th17-polarizing and nonpolarizing (Th0) conditions. ADAM8, 9, 10, 12, 15, 17, 19, 28, and 33 were chosen because they were reported to be expressed by immune cells in immune system–wide expression scans (9, 24). We found that several ADAM mRNAs, including ADAM8, 9, 10, 15, and 19 were expressed at significantly higher levels in Th17-polarized cells compared to nonpolarized Th0 cells (Fig. 1*A*). Among them, ADAM9 showed the highest expression levels in cells polarized under Th17 conditions. These results prompted us to consider that ADAM9 is important in Th17 cell differentiation.

Next, we assessed the impact of ADAM9 expression in T cells cultured under Th0, Th1, Th2, Th17, and Treg-polarizing conditions. We found that ADAM9 mRNA and protein levels were increased only when the cells were polarized toward Th17 rather than any of the other conditions (Fig. 1*B*). Time course data of ADAM9 mRNA expression in cells cultured under Th0- and Th17-polarizing conditions revealed that ADAM9 was expressed at the late phase of Th17-polarizing cultures (*SI Appendix*, Fig. S1). To investigate the importance of ADAM9 in Th17 cell differentiation, we generated lentivirus particles containing shRNA specific for ADAM9. Naïve $CD4^+$ T cells were cultured under Th17-polarizing conditions and were transfected with the ADAM9-targeting shRNA or with the control-scrambled shRNA. After confirming that the ADAM9-shRNA, but not the control shRNA, suppressed ADAM9 expression in Th17-polarized cells, we noted that suppression of ADAM9 expression reduced significantly Th17 cell differentiation among ADAM9-shRNA transfected cells compared to those that received control shRNA (Fig. 1*C*). Additionally, we generated an ADAM9 overexpression vector and transfected Th17-polarized cells with an empty or ADAM9 overexpression vector. After we confirmed that ADAM9 expression was increased in ADAM9 vector-transfected Th17-polarized cells, we found that the ADAM9-overexpressing cells displayed increased Th17 differentiation compared to cells transfected with the empty vector (Fig. 1*D*). Next, we assessed Th1, Th2, Th17, and Treg differentiation among cells obtained from *Adam9*-sufficient and -deficient mice and found that only Th17 cell differentiation was suppressed when *Adam9* was genetically absent (Fig. 2 *A*–*E* and *SI Appendix*, Fig. S2*A*). We also determined the expression of retinoic acid receptor-related orphan receptor gamma t (RORγt), the master transcription factor of Th17 cells, and found that the median fluorescence intensity (MFI) of RORγt was decreased in Th17 cells from *Adam9*-deficient mice (Fig. 2*F*). These data confirmed that ADAM9 is specifically expressed in Th17 cells, and it is requisite for Th17 cell differentiation.

ADAM9 Drives Th17 Cell Differentiation through the TGF-β1 Activation. Next, we set out to explore the molecular mechanisms whereby highly expressed ADAM9 promotes Th17 cell differentiation. TGF-β1 and IL-6 are essential in Th17 differentiation (7). TGF-β is secreted in a latent complex form, which consists of disulfide-linked homodimers complexed with the latency-associated peptide (LAP) (25). The latent TGF-β1 composed of the bioactive TGF-β1 and LAP needs to be activated prior to binding to the TGF-β receptor (26). Several matrix metalloproteinases (MMPs) including MMP2, MMP3, MMP9, and MMP13 have been reported to cleave LAP and activate TGF-β1 (27), but the expression levels of these mRNA are low in T cells (24). The disintegrin-like domain is a ligand for integrins, and it has been reported that the proteinase function of the metalloproteinase domain depends on the binding of the disintegrin domain to integrins (28). Because ADAM9 and LAP share the same integrin-binding ability (29, 30) and the two molecules come into physical proximity, we hypothesized that ADAM9 activates latent TGF-β1 by cleaving off LAP.

Accordingly, we cultured naïve $CD4^+$ T cells obtained from *Adam9*-sufficient or -deficient mice under Th17-polarizing conditions with latent TGF-β1(inactive) instead of bioactive TGF-β1. As shown in Fig. 2*D* and *SI Appendix*, Fig. S2*A*, Th17 differentiation was suppressed significantly in cells from *Adam9*-deficient mice compared to cells from *Adam9*-sufficient mice when cells were cultured with latent TGF-β1 instead of bioactive TGF-β1. Interestingly, when we cultured naïve T cells under Treg-polarizing conditions with latent TGF-β1, there was no significant difference in Treg differentiation between *Adam9*-sufficient and -deficient mice (Fig. 2*E*). Moreover, the MFI of RORγt was significantly decreased in Th17-polarized cells with latent TGF-β1 from *Adam9*-deficient mice (Fig. 2*F*). These results suggest that ADAM9 contributes to TGF-β1 activation by Th17 cells.

In addition, to assess whether ADAM9 affects IL-10 production by Th17 cells, we determined IL-10 production by $CD4^+$ cells cultured under Th17-polarizing conditions. We did not find a significant difference in IL-10 production by cells cultured under Th17-polarizing conditions in the presence of bioactive TGF-β1, whereas IL-10 production by Th17 cells generated from *Adam9*-deficient mice was significantly lower than that from cells from *Adam9*-sufficient mice cultured in the presence of latent TGF-β1. This finding supports a previous report that TGF-β1 is pivotal for IL-10 production by Th17 cells (31).

To confirm the ability of ADAM9 to activate TGF-β1, we conducted an enzymatic assay in which we incubated latent TGF-β1 with recombinant ADAM9 and observed that the concentration of LAP was clearly decreased (Fig. 3*A*). In addition, we assessed the enzymatic function of ADAM9 in a live cell setting. We cultured Th17 or Treg polarized cells with latent TGF-β1 and found that LAP levels in the culture supernatants were decreased in Th17 cells from *Adam9*-sufficient mice compared with cells from *Adam9*-deficient mice (Fig. 3 *B*, *Left*). However, the levels of LAP in the Treg cell culture conditions did not show significant differences between *Adam9*-sufficient and -deficient conditions (Fig. 3 *B*, *Right*).

To assess the TGF-β1 downstream signaling events, we examined the phosphorylation of SMAD2/3 under Th17-polarizing culture conditions with or without latent TGF-β1. TGF-β1 binding to the TGF-β type 1 receptor directly phosphorylates Ser465 and Ser467 of Smad2 and Ser423 and Ser425 of Smad3 (32, 33). Along with STAT3, the phosphorylated SMAD2 acts as the transcription factor and positively regulates the generation of Th17 cells through binding to the *RORC* promoter, which drives the expression of RORγt (34). As shown in Fig. 3*C*, the MFI of phosphorylated SMAD2/3 was diminished in cells from *Adam9*-deficient mice compared to cells from *Adam9*-sufficient mice. Collectively, we have confirmed that ADAM9 promotes Th17 differentiation through the activation of TGF-β1 and the subsequent phosphorylation of SMAD2.

Our data suggest that ADAM9 enhances the Th17 differentiation through TGF-β1 activation. However, since there is a difference in the Th17 differentiation between *Adam9*-sufficient and -deficient $CD4^+$ T cells cultured in the presence of bioactive TGF-β1 condition, we postulate that ADAM9 may have additional roles during the Th17 differentiation of $CD4^+$ T cells. To assess this, we conducted cultures under Th17-polarizing conditions using X-VIVO 15 media (serum-free media optimized for T cells) instead of the routinely used culture media (RPMI medium 1640 with 10% fetal bovine serum). Interestingly, there was a significant difference in Th17 differentiation between Adam9-sufficient $CD4^+$ T cells and -deficient cells cultured under Th17-polarizing conditions in X-VIVO serum-free media and latent TGF-β1—but not when cultured in the same medium in the presence of bioactive TGF-β1 (*SI Appendix*, Fig. S3). These results suggest that ADAM9 acts, besides activating TGF-β1, through additional

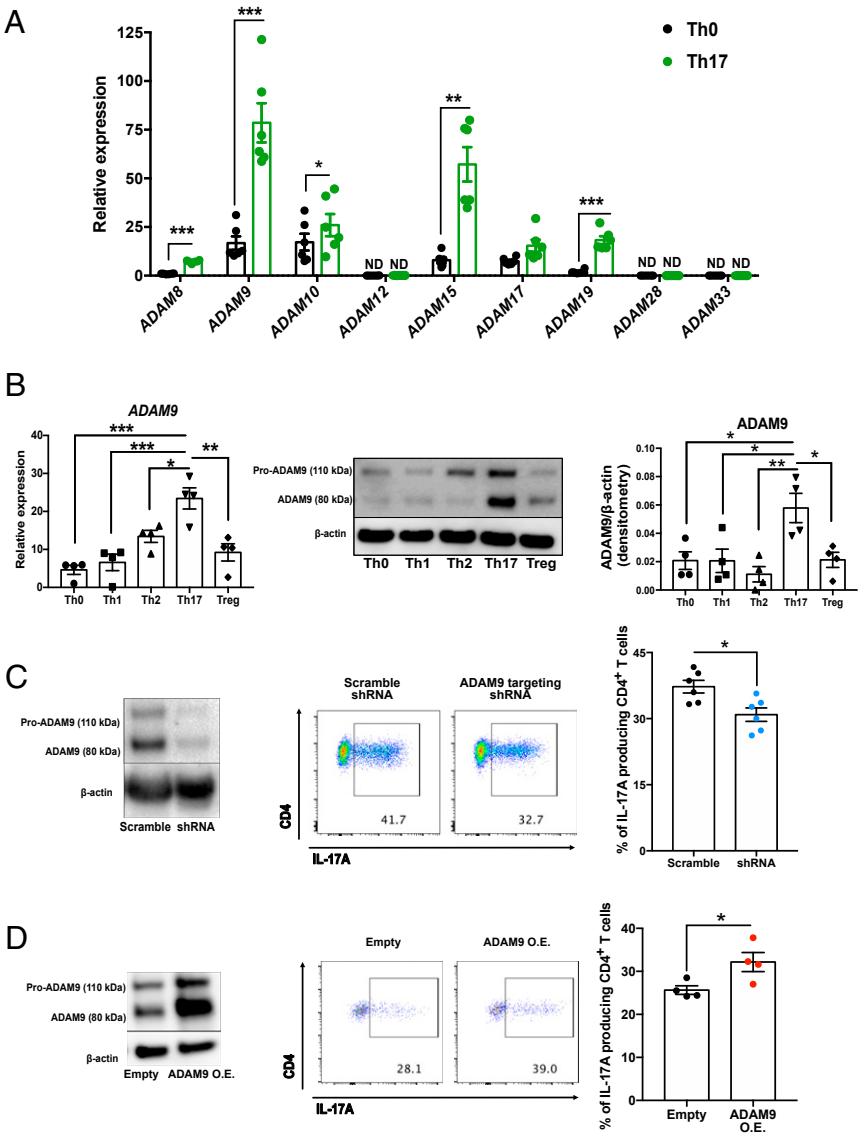

Fig. 1. ADAM9 is expressed by Th17 cells and promotes Th17 cell differentiation. (*A*) Gene expression (qRT-PCR) of members of the ADAM family in $CD4^+$ T cells cultured for 3 d under Th0 and Th17 conditions. Cumulative data are shown (mean ± SEM, $n = 6$). (*B*) Gene expressions (qRT-PCR) of ADAM9 in $CD4^+$ cells cultured under the indicated conditions. Cumulative data are shown (*Left*, mean ± SEM, $n = 4$). A representative Western blot of $CD4^+$ cells cultured for 3 d for pro-ADAM9, ADAM9 (active), and β-actin expressions are shown (*Center*), and cumulative densitometric readings of ADAM9 (active) and β-actin are shown (*Right*, mean ± SEM, $n = 4$). (*C*) Naive $CD4^+$ T cells were cultured under Th17-polarizing conditions and transfected with ADAM9-shRNA or scramble-shRNA as a negative control. Pro-ADAM9, ADAM9 (active), and β-actin protein expressions on day 3 were assessed by Western blotting. A representative (of three) blot is shown (*Left*). Representative flow plots (*Center*) and cumulative data (*Right*) are shown (mean ± SEM, $n = 6$). (*D*) Naive $CD4^+$ T cells were cultured under Th17-polarizing conditions and empty vector (empty) or ADAM9 overexpression (ADAM9 O.E.) plasmids were transfected into cultured T cells on day 1. Pro-ADAM9, ADAM9 (active), and β-actin protein expressions on day 3 were assessed by Western blotting. Representative (of three) blots are shown (*Left*). Representative flow plots (*Center*) on day 3 and cumulative data (*Right*) are shown (mean ± SEM, $n = 4$). $^*P < 0.05$, $^{**}P < 0.01$, $^{***}P < 0.001$, ND: not detected.

unknown factors present in the serum and relevant to Th17 differentiation.

ICER Promotes ADAM9 Expression in Th17 Cells. We have reported that inducible cAMP early repressor, one of the splice variants of the transcription factor cAMP response element modulator (CREM), is predominantly expressed in Th17 cells and drives Th17 cell differentiation (35). Since the putative CRE binding site exists in the promotor region of the *ADAM9* gene, which is well conserved in both humans and mice, we hypothesized that ICER/CREM promotes ADAM9 expression in Th17 cells. To assess this hypothesis, we compared ADAM9 expression in *ICER*/*CREM*-sufficient mice and -deficient mice and found that mRNA expression of ADAM9 was increased in Th17 cells from *ICER*/*CREM*-sufficient mice compared with cells from deficient mice (Fig. 4*A*). Additionally, ADAM9 protein also showed increased expression levels in Th17 cells from *ICER*/*CREM*-sufficient mice compared with cells from deficient mice (Fig. 4*B*). To confirm that ADAM9 is induced in IL-17A–producing cells only from *ICER*/*CREM*-sufficient mice, we cultured T cells from B6.IL-17GFP *ICER*/*CREM*-sufficient mice and -deficient mice under the same Th17 culture conditions and sorted green fluorescent protein (GFP)-positive (IL-17A–producing) cells. As shown in Fig. 4*C*, ADAM9 mRNA expression in IL-17A–producing cells was enriched in cells from *ICER*/*CREM*-sufficient mice compared with cells from deficient mice. Previously we had shown that ICER/CREM is induced by

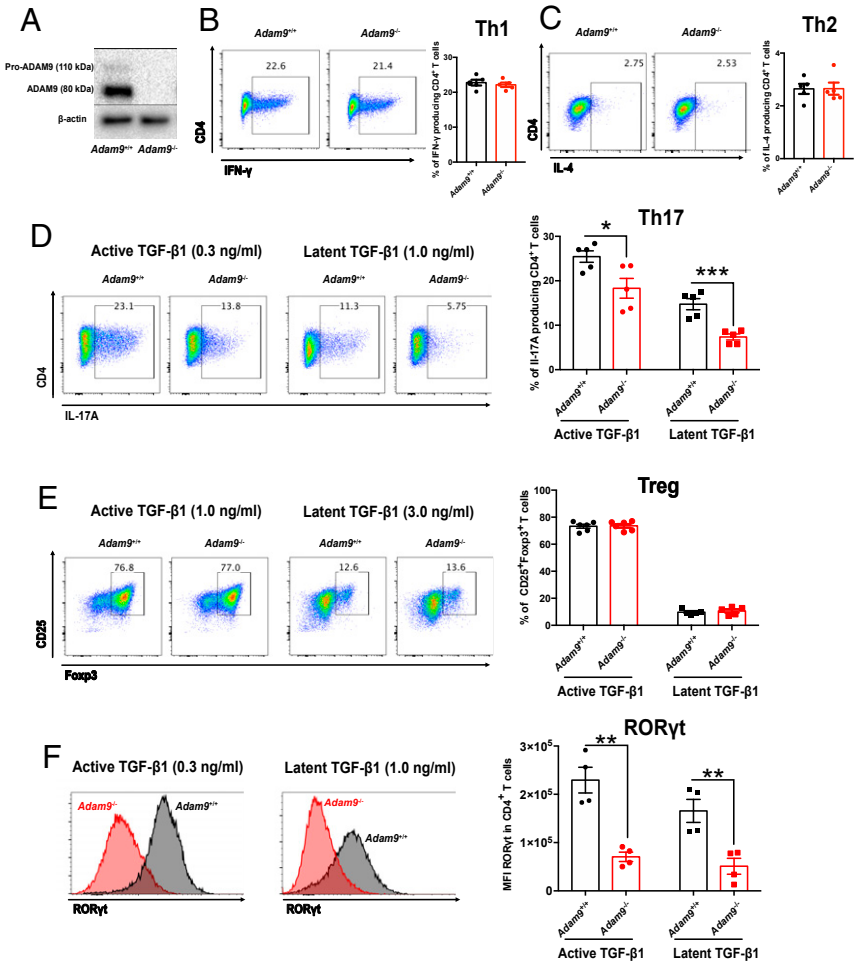

Fig. 2. Genetic ADAM9 deficiency results in decreased Th17 cell differentiation. (*A–F*) Naïve CD4$^+$ T cells from B6. *Adam9*$^{+/+}$ mice or B6. *Adam9*$^{-/-}$ mice were polarized for 3 d under the indicated conditions. (*A*) Pro-ADAM9, ADAM9 (active), and actin protein expressions were assessed on day 3 by Western blotting. A representative (of three) blot is shown. (*B–E*) Representative flow plots of intracellular expressions of IFNγ, IL-4, IL-17A, and Foxp3 (*Left*) of cells cultured under the indicated conditions and cumulative data (*Right*) are shown (mean ± SEM, $n = 5$). (*F*) Representative flow histogram (*Left*) and cumulative MFI of RORγt (*Right*) are shown (mean ± SEM, $n = 4$). $^*P < 0.05$, $^{**}P < 0.01$, $^{***}P < 0.001$.

IL-6 through STAT3 signaling (35), and accordingly, the IL-6/STAT3 axis should be able to induce ADAM9 expression through ICER/CREM induction. To evaluate this, we analyzed ADAM9 expression in Th17 polarized cells cultured with or without STAT3 inhibitor and found that the STAT3 inhibitor reduced ADAM9 expression in Th17 polarized cells (Fig. 4*D*). We have reported that Th17 polarized cells from *ICER/CREM*-deficient mice show decreased production of IL-17A (35). Forced overexpression of ADAM9 in Th17-polarized cells from *ICER/CREM*-deficient mice showed a recovery of IL-17A production (Fig. 4*E*). These findings suggest that ICER/CREM promotes ADAM9 expression in Th17 polarized cells.

Further, we asked whether ICER/CREM can induce ADAM9 expression directly by binding to the *ADAM9* promoter that defines a CRE. We constructed luciferase reporter vectors driven by the full-length *ADAM9* promoter or by the *ADAM9* promoter, in which the CRE (Δ-134/130) had been mutated (Fig. 4*F*). The *ADAM9* promoter-reporter activity in *ICER/CREM*-sufficient mice was decreased in the Th17-polarized cells transfected with the mutated vector compared with those transfected with the reporter vector with the full *ADAM9* promoter (Fig. 4*G*). Moreover, the *ADAM9* promoter activity was decreased in *ICER/CREM*-deficient cells with full-length *ADAM9* promoter compared to *ICER/CREM*-sufficient cells transfected with full-length *ADAM9* promoter-reporter. To confirm that ICERγ (the most dominant isoform of ICER) accessed the *ADAM9* promoter at the CRE site, we transfected a Flag-tagged ICERγ overexpression vector into Th17-polarized *ICER/CREM*-deficient T cells and measured the recruitment of ICERγ to the *ADAM9* promoter using chromatin immunoprecipitation (ChIP) assays. ICERγ accumulated at the promoter region of *ADAM9*, which contains the CRE. However, there was low accumulation at the exon1 region of *ADAM9* and the intron3 region of the other gene *(Tm2d2)* located next to *ADAM9*, which also contains a putative CRE, suggesting that ICERγ selectively accumulates at the promoter region of *ADAM9* in Th17-polarized T cells (Fig. 4*H*). In addition, we conducted ChIP assays to assess RORγt accumulation in the same, but, as shown in *SI Appendix*, Fig. S4, we found none. These data confirm that the transcription factor ICER induces ADAM9 expression by binding directly to the *ADAM9* promoter in Th17 cells.

Deletion of *ADAM9* Ameliorates EAE. Our in vitro data suggest that ADAM9 can serve as a therapeutic target for Th17-dependent autoimmune diseases. To assess this, we used EAE, a well-established Th17-related autoimmune disease model. *Adam9*-deficient mice displayed a significantly reduced clinical score compared with *Adam9*-sufficient mice (Fig. 5*A*). Histology scores of spinal cords were significantly decreased in the *Adam9*-deficient mice compared

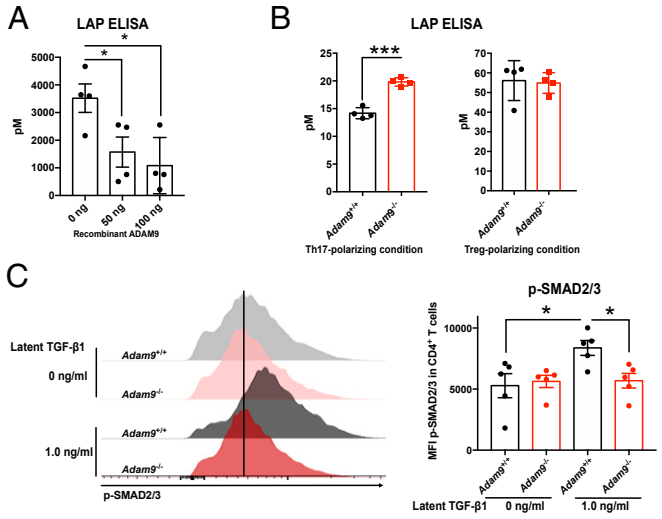

Fig. 3. ADAM9 drives Th17 cell differentiation through the TGF-β1 activation. (*A*) Recombinant ADAM9 or buffer alone were incubated with 50 ng of latent TGF-β1 at 37° C for 16 h at pH 7.4. The reaction products which contain latency-associated peptide (LAP) were analyzed by ELISA kit for detecting LAP (mean ± SEM, $n = 4$). (*B*) Naïve CD4$^+$ T cells were cultured under Th17 or Treg conditions. After 48 h of incubation, culture media were changed to the Th17-polarizing conditions with latent TGF-β1 (1.0 ng/mL) or Treg-polarizing conditions with latent TGF-β1 (3.0 ng/mL), respectively. After 16 h of incubation, the concentration of LAP in the supernatants was determined by ELISA (mean ± SEM, $n = 4$). (*C*) Naïve CD4$^+$ T cells were cultured under the Th17 condition with latent TGF-β1 (1.0 ng/mL). After 48 h of incubation, culture media was changed to the Th17-polarizing condition with latent TGF-β1 (1.0 ng/mL or 0 ng/mL as a control), but without FBS to make serum-starved condition. After 16 h of incubation with the serum-starved condition, cells were analyzed by flow cytometry to assess p-Smad2/3. Representative flow histogram (*Left*) and cumulative MFI of phosphorylated SMAD2/3 (*Right*) are shown (mean ± SEM, $n = 5$). *$P < 0.05$, ***$P < 0.001$.

to the *Adam9*-sufficient mice (Fig. 5*B*). This observation was further confirmed by assessing the absolute numbers of spinal cord-infiltrating cells by flow cytometry. Cells from *Adam9*-deficient mice showed reduced numbers of CD4$^+$ T cells (CD45$^+$ CD90.2$^+$ CD4$^+$), IL-17A (CD45$^+$ CD90.2$^+$ CD4$^+$ IL-17A$^+$), and IFNγ-producing CD4$^+$ T cells (CD45$^+$ CD90.2$^+$ CD4$^+$ IFNγ$^+$) in the spinal cord compared with those of *Adam9*-sufficient mice (Fig. 5*C*). However, there was no significant difference in the number of spinal cord-infiltrating Treg (CD45$^+$ CD90.2$^+$ CD4$^+$ CD25$^+$ FOXP3$^+$) cells between the *Adam9*-sufficient and -deficient groups of mice (Fig. 5*C*).

Next, we immunized *Adam9*-sufficient and -deficient mice with $MOG_{35–55}$, and the draining lymph nodes were extracted on day 8. Isolated cells from the lymph nodes were further cultured in ex vivo with MOG for 3 d. IL-17A and IFNγ concentrations were measured by enzyme-linked immunosorbent assay (ELISA). As shown in Fig. 5*D*, IL-17A and IFNγ production was decreased in *Adam9*-deficient mice.

To further investigate the physiological significance of ADAM9 in a Th17 cell-specific manner, we performed an adoptive transfer EAE experiment in which we prepared in vitro Th17-polarized cells delivered from *Adam9*-sufficient or -deficient 2D2 mice and transferred them into *Rag1*$^{-/-}$ mice. Mice that received *Adam9*-deficient 2D2 Th17-polarized cells had reduced EAE disease compared with those who received cells from *Adam9*-sufficient 2D2 mice (Fig. 5*E*). We confirmed the effect of ADAM9 deletion by assessing the absolute numbers of spinal cord-infiltrating cells by flow cytometry. *Rag1*$^{-/-}$ mice, which received Th17-polarizing cells from *Adam9*-deficient 2D2 T cells, had reduced numbers of CD4$^+$ T cells, and IL-17A–producing CD4$^+$ T cells in the spinal cord compared with those from *Adam9*-sufficient 2D2 mice (Fig. 5*F*). Furthermore, to assess whether ADAM9 acts on antigen presenting cells (APCs) in addition to T cells, we cocultured APCs and CD4$^+$ T cells obtained from *Adam9*-sufficient and/or *Adam9*-deficient mice. The percentage of IL-17–producing CD4$^+$ T cells was found to be similar regardless of the presence or absence of ADAM9 in APCs (*SI Appendix*, Fig. S5). These results confirmed that ADAM9 deletion ameliorates EAE in a Th17-cell–dependent manner.

CRISPR/Cas9 Deletion of ADAM9 Reduces Th17 Cell Differentiation in T Cells from Patients with SLE. We have established that ICER levels are increased in CD4$^+$ T cells from SLE patients, and that this promotes Th17 cell differentiation (35). We considered that ICER/CREM may induce ADAM9 expression, which promotes Th17 cell differentiation in SLE patients. To demonstrate that this pathway operates in T cells from patients with SLE, we isolated CD4$^+$ T cells from SLE patients and age-, sex-, and ethnicity-matched healthy individuals and stimulated them with CD3 and CD28 antibodies. As shown in Fig. 6*A*, ADAM9 expression is enriched in CD4$^+$ T cells from SLE patients compared to cells from healthy individuals. We also compared ADAM9 expression in CD4$^+$ T cells from patients with low and high SLE Disease Activity Index (SLEDAI) and found that there was no significant difference between the two groups (*SI Appendix*, Fig. S6*A*). We sorted peripheral blood mononuclear cells from healthy individuals and SLE patients into naïve CD4$^+$ T cells, memory Th17 cells, and memory non-Th17 cells by flow cytometry (*SI Appendix*, Fig. S6*B*) and analyzed the relative expression of *ADMA9* mRNA. We found that the ADAM9 expression levels in Th17 cells from SLE were significantly higher than in naïve cells (*SI Appendix*, Fig. S6*C*). Finally, to elucidate the role of ADAM9 for Th17 cell differentiation in CD4$^+$ T cells in human autoimmune disease, we deleted *ADAM9* in CD4$^+$ T cells from SLE patients using the CRISPR/Cas9 gene-editing system. Indeed, IL-17A production by *Adam9*-deficient cells cultured under Th17-polarizing conditions was decreased (Fig. 6*B*). The similar result was found by using primary CD4$^+$ T cells obtained from healthy individuals (*SI Appendix*, Fig. S6*D*). These results demonstrate that ADAM9 promotes Th17 cell differentiation in human CD4$^+$ T cells and may drive autoimmunity in humans.

Discussion

Today there has been scant information on the role of ADAM molecules in the control of immune cell function. ADAM12 has been reportedly enriched in both human Treg and CCR6$^+$ Th17 cells (36), and ADAM17 was claimed not to be involved in IL-17 production (37). In the present study, we identified that ADAM9 is enriched in Th17 cells and drove their differentiation. Mechanistically, we demonstrated that the transcription factor ICER/CREM induces ADAM9 expression in Th17 cells, and that ADAM9 cleaved off LAP, a component of latent TGF-β1, to activate TGF-β1. At the translational level, genetic deletion of ADAM9 suppressed EAE in mice and the generation of Th17 from CD4$^+$ T cells from patients with SLE.

Th17 cell polarization condition requires TGF-β1 and IL-6, while Treg cell polarization requires TGF- β1 and IL-2. In addition to the paracrine-secreted TGF-β1, TGF-β1 is highly expressed by Th17 cells, and it acts in an autocrine manner to maintain Th17 cells (38). Recently, it was claimed that high amounts of glucose promote Th17 differentiation by generating reactive oxygen species, which produce bioactive TGF-β1 through an unknown mechanism (39). Our study assigns a distinct proteinase ADAM9-mediated activity in the production of active TGF-β1.

Interestingly, ADAM9 did not appear to have a role in Treg differentiation. Since our data showed that the expression of ADAM9 is low in Treg cells, we speculated that Treg cells may not be able to activate TGF-β1 by themselves regardless of the

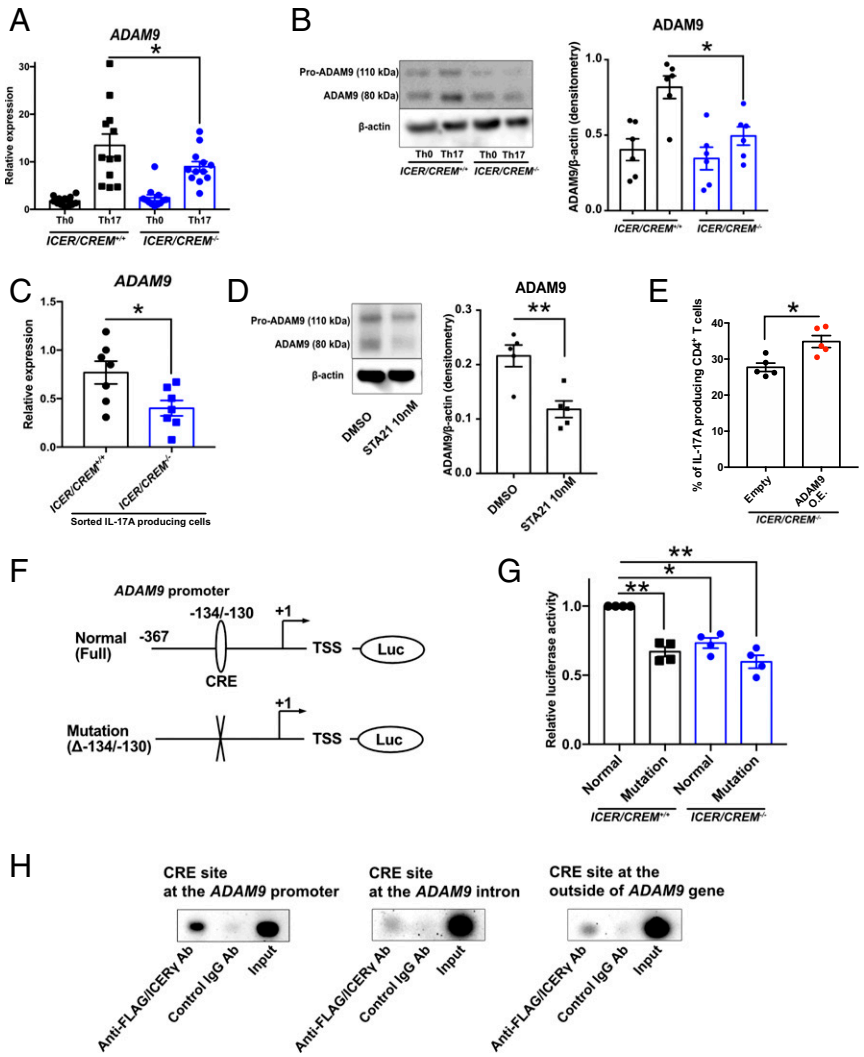

Fig. 4. Transcriptional factor ICER promotes ADAM9 expression in Th17 cells. (*A* and *B*) *ICER/CREM*-deficient or -sufficient naïve CD4$^+$ T cells cultured under Th17-polarizing conditions for 3 d. (*A*) Relative ADAM9 mRNA expressions were assessed by qRT-PCR. Cumulative data are shown (mean ± SEM, $n = 12$). (*B*) Pro-ADAM9, ADAM9 (active), and β-actin expressions on day 3 were determined by Western blotting. A representative (of six) blot is shown (*Left*) and cumulative densitometric readings of ADAM9 (active) and β-actin are shown (*Right*) (mean ± SEM, $n = 6$). (*C*) Naïve CD4$^+$ T cells from *ICER/CREM*-deficient or -sufficient IL-17GFP mice were polarized under Th17 conditions for 3 d. ADAM9 mRNA expression of FACS-sorted GFP$^+$ cells (IL-17A–producing cells) was assessed by qRT-PCR (mean ± SEM, $n = 7$). (*D*) Th17-polarized naive CD4$^+$ T cells were cultured in the presence of a STAT3 inhibitor (STA21, 10 μM) or dimethyl sulfoxide (DMSO) for 3 d. Pro-ADAM9, ADAM9 (active), and β-actin expressions were determined by Western blotting. A representative (of five) blot is shown (*Left*) and cumulative densitometric readings of ADAM9 (active) and β-actin are shown (*Right*) (mean ± SEM, $n = 5$). (*E*) Naive CD4$^+$ T cells from *ICER/CREM*-deficient IL-17GFP mice were cultured under Th17-polarizing conditions and empty vector (empty) or ADAM9 overexpression (ADAM9 O.E.) plasmids were transfected into cultured T cells on day 1. Representative flow plots on day 3 (*Left*) and cumulative data (*Right*) are shown (mean ± SEM, $n = 5$). (*F–H*) ICERγ binds to the *ADAM9* promoter directly and increases its activity. *ICER/CREM*-deficient or -sufficient naïve CD4$^+$ T cells were cultured under Th17-polarizing conditions. (*F*) Schematic representation of the used reporter constructs. Numbers represent the position from the transcription start site of the murine *ADAM9* gene. (*G*) The full-length *ADAM9* promoter region (full) or a version containing a mutated CRE binding site (Δ-134/-130) were transfected into Th17-polarized T cells on day 1. Cells were harvested and lysed on day 2. Cumulative results of four independent experiments are shown (mean ± SEM). (*H*) The FLAG-tagged ICERγ overexpression vector was transfected into *ICER/CREM*-deficient CD4$^+$ T cells on day one. Cells were harvested and lysed on day 3, and binding of FLAG/ICERγ to the CRE was assessed by ChIP assay. CRE at the intron1 of the ADAM9 gene and CRE at the intron 3 of the adjacent gene *(Tm2d2)* were used as negative controls for ChIP enrichment. Representative blots from three experiments are shown. $*P < 0.05$, $**P < 0.01$.

presence or absence of ADAM9, and the needed TGF-β1 is generated by other cells or through other mechanisms.

Previously, we had demonstrated that the levels of the transcriptional repressor isoform of CREM (CREMα) are increased in T cells from patients with SLE and induce IL-17 production by keeping the locus open through epigenetic mechanisms (40, 41). Moreover, ICER, a small splice variant of CREM, the expression of which is driven by an alternative P2 promoter, is expressed in murine and human Th17 cells and drives Th17 cell differentiation by binding to the *Il17a* promoter (35). Here we have demonstrated that while ICER/CREMα promotes the transcription of *IL17,* it also binds to the promoter of *ADAM9* and induces its expression, thus adding a mechanism whereby ICER/CREM promotes the generation of Th17.

With the prospect of developing ADAM9 inhibitors (42), the identified role of ADAM9 in the expression of the Th17-dependent EAE pathology and the generation of Th17 cells from CD4$^+$ cells from patients with SLE has a significant translational impact. Here we found CD4$^+$ cells from patients with SLE to have increased levels of ADAM9: a finding that corroborates reports of increased

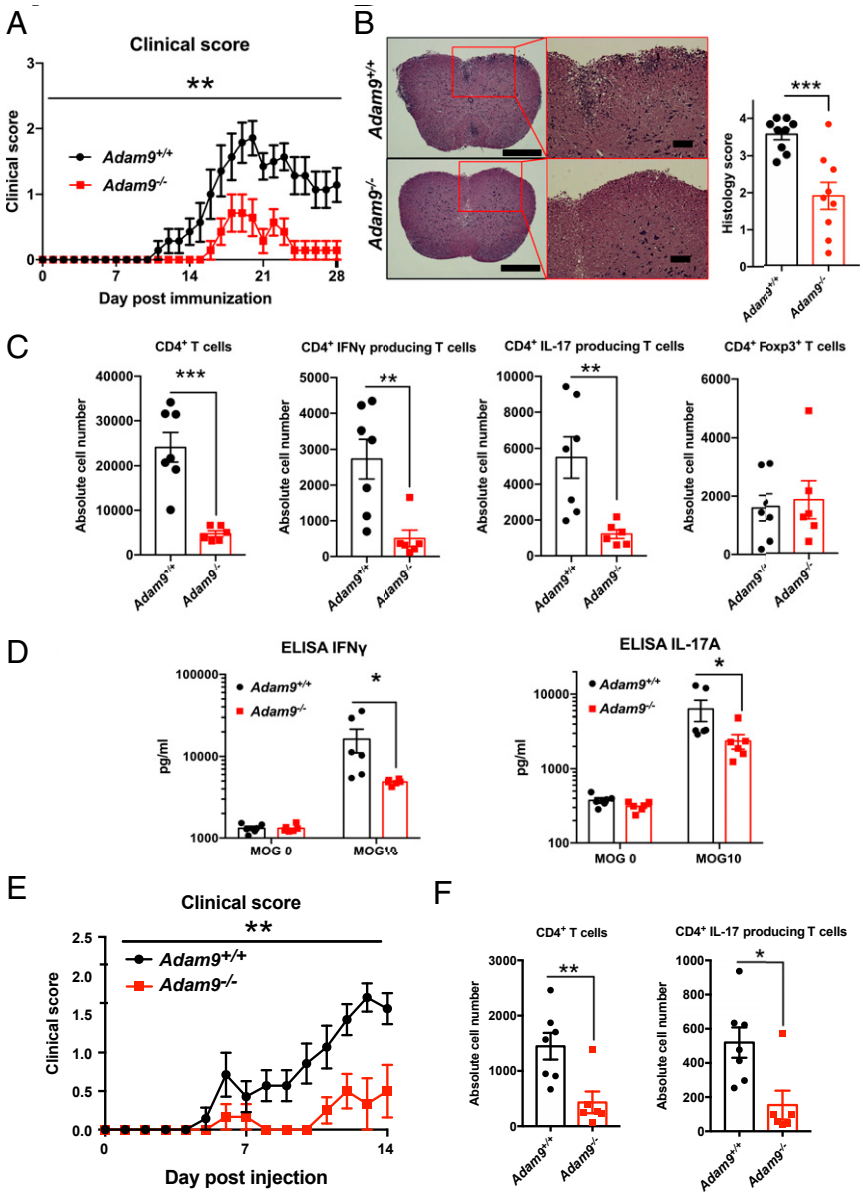

Fig. 5. ADAM9 deletion mitigates EAE. (*A–D*) EAE was induced in B6. ADAM9$^{+/+}$ mice or B6. *Adam9*$^{-/-}$ mice by immunization with $MOG_{35–55}$ emulsified in the complete Freund's adjuvant. (*A*) Clinical scores. Cumulative results of two independent experiments are shown (mean ± SEM, $n = 7$). (*B*) Spinal cords were harvested on day 14 and stained with H&E to assess inflammation (scale bars, 500 μm or 100 μm [magnified panels]). Quantitative cumulative data are shown on the right (mean ± SEM, $n = 9$. (*C*) Absolute cell numbers of spinal cord–infiltrated CD4$^+$ T cells, IL-17A–producing CD4$^+$ T cells, IFNγ-producing CD4$^+$ T cells, and Foxp3$^+$ CD4$^+$ T cells were evaluated by flow cytometry on day 14. Cumulative data are shown (mean ± SEM, $n = 7$). (*D*) Mononuclear cells harvested from inguinal lymph nodes on day 8 were activated in vitro with $MOG_{35–55}$ for 3 d. IL-17A and IFNγ concentrations were measured by ELISA. Cumulative data are shown (mean ± SEM, $n = 6$). (*E* and *F*) Naïve CD4$^+$ T cells from *Adam9*$^{+/+}$ 2D2 mice or *Adam9*$^{-/-}$ 2D2 mice were cultured under Th17-polarizing conditions. On day 3 of culture, harvested cells were transferred to recipient *Rag*$^{-/-}$ mice intravenously. (*E*) Clinical scores of recipient mice. Cumulative results of six to seven mice per group are shown (mean ± SEM). (*F*) Absolute cell numbers of spinal cord–infiltrated CD4$^+$ T cells and IL-17A–producing CD4$^+$ T cells were evaluated by flow cytometry on day 14. Cumulative data are shown (mean ± SEM, $n = 6$-7). *$P < 0.05$; **$P < 0.01$, ***$P < 0.001$.

ADAM9 mRNA expression in peripheral blood mononuclear cells (43) and the urine of patients with lupus nephritis (44). We provide a definitive role for ADAM9 in the generation of Th17 cells by showing that its genetic deletion of SLE T cells limits their development.

In sum, we have identified ADAM9 as a proteinase that drives Th17 cell differentiation without affecting the development of other T cell lineages. More precisely, we show that ICER/CREM promotes the expression of ADAM9, which, through its proteinase activity, enables the production of active TGF-β1, a molecule required for Th17 differentiation. The demonstrated importance of ADAM9 in the development of EAE in mice and Th17 cells in patients with SLE will direct efforts to develop inhibitors of ADAM9 to treat diseases that engage Th17 cells in the development of pathology.

Materials and Methods

Human Samples and Cell Lines. Patients who fulfilled the criteria for the diagnosis of SLE as set forth by the American College of Rheumatology (45) and healthy individuals were enrolled. The Beth Israel Deaconess Medical Center Institutional Review Board approved the study protocol (2006-P-0298). Informed consent was obtained from all study subjects. The disease activity for each patient was calculated using the clinic-laboratory index SLEDAI (46). Age-, sex- and ethnicity-matched healthy individuals were chosen as controls for determining the expression of ADAM9 by Western blotting for Fig. 6*A*.

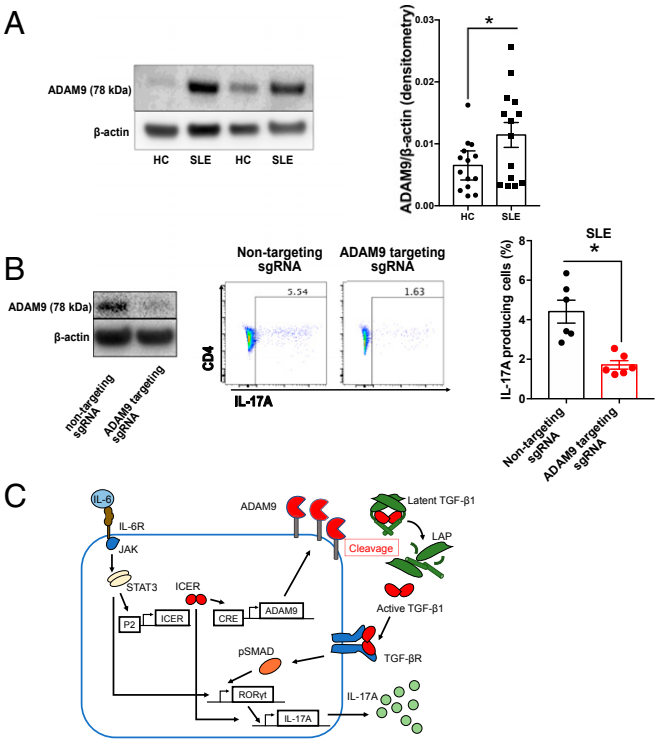

Fig. 6. ADAM9 highly expressed in CD4$^+$ T cells from SLE patients and promoted Th17 differentiation. (*A*) Purified CD4$^+$ T cells from healthy controls (HC) and SLE patients were stimulated with plate-bound CD3 and CD28 antibodies. After overnight (14–16 h) stimulation, cells were collected, and ADAM9 and actin expressions were examined by Western blotting. A representative (n = 14) blot is shown (*Left*), and densitometric readings from cumulative data are shown on the *Right* (mean ± SEM, n = 14). (*B*) Naive CD4$^+$ T cells from SLE patients were cultured under Th17-polarizing conditions and nontarget sgRNA or ADAM9-targeting sgRNA along with Cas9 protein were transfected on day 2. A representative (n = 3) blot, which confirmed the efficient deletion of ADAM9, is shown on the *Left*. Representative flow plots on day 7 (*Center*) and cumulative data (*Right*) are shown (mean ± SEM, n = 6). (*C*) A proposed model represents that ADAM9 drives Th17 cell differentiation through the activation of TGF-β1.

Research subject information is shown in *SI Appendix*, Tables S1–S3. Peripheral venous blood was collected in heparin-lithium tubes, and total human CD4$^+$ T cells were purified by using a magnetic cell-sorting human CD4$^+$ T cell isolation kit (Miltenyi Biotec), and human naïve CD4$^+$ T cells were purified by using a magnetic cell-sorting human naïve CD4$^+$ T cell isolation kit (Miltenyi Biotec). These protocols use a negative selection procedure that produces >95% pure CD4$^+$ or naïve CD4$^+$ T cells as tested by fluorescence-activated cell-sorting analysis. HEK-293T cells were purchased from American Type Culture Collection (ATCC) and have been tested for mycoplasma by ATCC.

Mice. SV129/Bl6.*ICER/CREM*$^{-/-}$mice were obtained from Günther Schütz (Das Deutsche Krebsforschungszentrum, Heidelberg, Germany) (47). Animals were crossed to C57BL/6J mice for over nine generations to transfer the *ICER/CREM*$^{-/-}$ locus to the B6 background. *Adam9*$^{-/-}$ mice in a pure C57BL/6 background were obtained from Caroline Owen (Brigham and Women's Hospital, Boston, MA) (48). C57BL6J mice, C57BL/6- Il17atm1Bcgen/J (IL-17GFP) mice, C57BL/6-Tg(Tcra2D2, Tcrb-2D2)1Kuch/J (2D2), and B6.129S7-Rag1tm1-Mom/J (Rag1-KO) mice were purchased from The Jackson Laboratory. B6.*ICER/CREM*$^{-/-}$.IL-17GFP mice were made by crossing B6.*ICER/CREM*$^{-/-}$ mice with IL-17GFP mice. 2D2.*Adam9*$^{-/-}$ mice were made by crossing *Adam9*$^{-/-}$ mice with 2D2 mice. Animals were killed at 8 to 12 wk of age for in vitro experiments and indicated number of weeks for in vivo experiments. All mice were maintained in a specific pathogen-free animal facility (BIDMC). Experiments were approved by the Institutional Animal Care and Use Committee of BIDMC.

Single-Cell Isolation. Spleens and lymph nodes were excised, and single-cell suspensions were obtained. Infiltrating lymphocytes in spinal cords were isolated as previously described (49). Spinal cords were digested with collagenase type IV (100 μg/mL) in Hanks' Balanced Salt Solution for 20 min (37 °C). Cell suspensions from digested spinal cords were subjected to density separation using Optiprep density gradient medium (Sigma-Aldrich) followed by flow cytometry.

In Vitro T Cell Differentiation. Murine naive CD4$^+$ T cells were purified using the mouse CD4$^+$ CD62L$^+$ T Cell Isolation Kit II (Miltenyi Biotec). Purified naive T cells in RPMI medium 1640 with 10% fetal bovine serum, penicillin-streptomycin, and 2-mercaptoethanol were stimulated with plate-bound goat anti-hamster antibodies, soluble anti-CD3 (0.25 μg/mL, 145-2C11; BioLegend), and anti-CD28 (0.5 μg/mL, 37.51; Bio X Cell) at 37 °C for Th0-nonpolarized condition culture. In addition to Th0-nonpolarizing conditions, the following stimulations were used for each polarizing condition: IL-12 (20 ng/mL, R&D Systems) and anti-IL-4 (10 μg/mL, C17.8; Bio X Cell) for Th1 condition; IL-4 (100 ng/mL, R&D Systems) and anti-IFNγ (10 μg/mL, XMG1.2; Bio X Cell) for Th2 condition; IL-6 (3 ng/mL, R&D Systems), TGF-b1 (0.3 ng/mL, R&D Systems), anti-IL-4 (10 μg/mL) and anti-IFNγ (10 μg/mL) for Th17; IL-6 (3 ng/mL), latent TGF-b1 (1.0 ng/mL, R&D Systems), anti-IL-4 (10 μg/mL) and anti-IFNγ (10 μg/mL) for Th17 with latent TGF- β1 condition; and IL-2 (20 ng/mL, R&D Systems), TGF-β1 (1.0 ng/mL, R&D Systems), anti-IL-4 (10 μg/mL) and anti-IFNγ (10 μg/mL) for Tregs condition; and IL-2 (20 ng/mL), latent TGF-β1 (3.0 ng/mL), anti-IL-4 (10 μg/mL) and anti-IFNγ (10 μg/mL) for Tregs with latent TGF-β1 condition. For signal transduction studies, STA21 (STAT3 inhibitor, Santa Cruz Biotechnology) was added to cultures on day 0. For the human Th17-polarized culture, isolated naive CD4$^+$ T cells in RPMI medium 1640 with 10% fetal bovine serum plus penicillin-streptomycin were stimulated with plate-bound anti-CD3 Ab (1 μg/mL, OKT-3; Bio X Cell), anti-CD28 Ab (1 μg/mL, CD28.2; BioLegend), IL-6 (50 ng/mL, BioLegend), TGF-β1 (10 ng/mL, BioLegend), IL-1β (10 ng/mL, BioLegend), IL-23 (50 ng/mL, BioLegend), anti-IL-4 Ab (10 μg/mL, Bio X Cell), and anti-IFN-γ Ab (5 μg/mL, B27; BioXCell) at 37 °C. X-vivo 15 medium (Lonza) was used for serum-free experiments in *SI Appendix*, Fig. S3.

APC/T Cell Coculture. CD11c$^+$ APCs were isolated using the CD11c MicroBeads (Miltenyi Biotec). Naïve CD4$^+$ T cells (3×10^5) and CD11c$^+$ APCs (3×10^4) from B6. Adam9$^{+/+}$ mice and/or B6. Adam9$^{-/-}$ mice were cultured for 3 d under Th17-polarizing conditions with bioactive TGF-β1 (0.3 ng/mL) or latent TGF-β1 (1.0 ng/mL).

ELISA. ELISA MAX Deluxe SET Mouse IL-17A (BioLegend), ELISA MAX Deluxe SET Mouse IFN-γ (BioLegend), Human Latent TGF-beta 1 ELISA Kit (STEMCELL Technologies) were used. All procedures were performed according to the manufacturer's instructions. Each assay was performed in duplicate independently.

RNA Isolation and Quantitative PCR. TRIzol reagent was used for RNA preparation. The following TaqMan probes (Thermo Fisher Scientific) were used to detect target genes in mice: *adam8* Mm01163449_g1, *adam9* Mm01218460_m1, *adam10* Mm00545742_m1, *adam12* Mm00475719_m1, *adam15* Mm00477328_m1, *adam17* Mm00456428_m1, *adam19* Mm00477337_m1, *adam28* Mm00456640_m1, *adam33* Mm00459691_m1, *tbp* (TATA box-binding protein) Mm00446973_m1, and *gusb* (β-glucuronidase) Mm01197698_m1. Gene expression was assessed by the comparative cycle threshold (CT) method and normalized to the reference genes *tbp* and *gusb* (50).

Western Blotting. Cell lysate was separated on NuPAGE 4–12% Bis-Tris Gel (Thermo Fisher Scientific), and proteins were transferred to a nitrocellulose membrane. The following antibodies were used: anti-ADAM9 ectodomain antibody (Catalog# AF949, R&D Systems, 1μg/mL), anti-b-actin antibody (clone AC-74, Sigma-Aldrich, 1:10,000), rabbit anti-goat IgG horseradish peroxidase (HRP)-conjugated antibody (Catalog# HAF017, R&D Systems, 1:1,000), and goat anti-mouse IgG HRP-conjugated antibody (Catalog# ab6789, Abcam, 1:3,000). The ECL system (Cytiva) was used for detection. Bands on blots corresponding to proteins of interest were analyzed by Image J software (NIH).

Flow Cytometry. The following antibodies were used for flow cytometry analysis: for mice, CD25 (clone PC61, 1:100), CD45 (clone 30-F11, 1:100), CD90.2 (clone 53-2.1, 1:100), IL-17A (clone JC11-18H10.1, 1:50), IL-4 (clone 11B11, 1:50), and IL-10 (clone JES5-16E3, 1:50) were purchased from BioLegend. CD4 (clone GK1.5, 1:100), RORγt (clone B2D, 1:100), IFNγ (clone XMG1.2, 1:50), and Foxp3 (clone FJK-16s, 1:100) were purchased from Thermo Fisher Scientific. For humans, CD3 (clone UCHT1, 1:100), IL-17A (clone BL168, 1:50), CD45RA (clone HI100, 1:100), CD25 (clone BC96, 1:100), CD127 (clone A019D5, 1:100), CCR4 (clone L291H4, 1:100), and CCR6 (clone G034E3, 1:100) were purchased from BioLegend. CD4 (clone SK3, 1:100) was purchased from Thermo Fisher Scientific. Zombie Aqua Fixable Viability Kit staining was performed to eliminate

dead cells (BioLegend). Surface staining was performed on ice for 20 to 30 min. Absolute cell numbers were calculated on the basis of the percentage of each cell population. For intracellular staining, collected cells were stimulated for 4 h in the culture medium with phorbol myristate acetate (500 ng/mL, Sigma-Aldrich), ionomycin (1.4 μg/mL, Sigma-Aldrich), and monensin (1 μL/mL, BD Biosciences), except for the detection of Foxp3 and RORγt. Cytofix/Cytoperm and Perm/Wash buffer (BD Biosciences) were used for fixation and permeabilization. All flow cytometry data were acquired on a Cytoflex LX (Beckman Coulter) and analyzed with FlowJo (BD Biosciences). BD FACS Aria II (BD Biosciences) was used for cell sorting. For ADAM9 overexpression experiments under Th17-polarized condition in murine primary T cells, IL-17GFP mice were used. All procedures were performed according to the manufacturer's instructions.

pSMAD2/3 Phospho-Flow Cytometry for Mouse Th17 Polarized Cells with Latent TGFb1. Purified naive murine CD4$^+$ T cells were cultured under Th17 conditions with latent TGF-β1 (1.0 ng/mL). After 48 h of incubation, cells were washed once with phosphate-buffered saline (PBS) and were changed to the Th17-condition media with latent TGF-β1 (1.0 ng/mL or 0 ng/mL as a control), but without fetal bovine serum (FBS) to facilitate a serum-starved condition. After overnight incubation in the serum-starved condition, cells were fixed and permeabilized by using Lyse/fix buffer and Perm buffer III (BD Biosciences). Cells were stained with mouse anti-Smad2 (pS465/pS467)/Smad3 (pS423/pS425) antibodies (BD Biosciences, clone: O72-670, 1:20) and cells surface antibodies for 30 min at room temperature.

Transfection of Overexpression Vectors. For ADAM9 overexpression, the mouse ADAM9 sequences were subcloned into the pIRES2-DsRed-Express vector by GenScript. All constructs were verified by DNA sequencing. For ADAM9 overexpression experiments in murine primary T cells, cells were harvested 1 d after starting culture, and empty vector or ADAM9 overexpression vector plasmid were transfected using the Amaxa Mouse T Cell Nucleofector Kit with the X-001 program (Lonza). The efficiency of the transfection in primary T cells was tested by flow cytometry as DsRED$^+$ cells and always exceeded 20%.

Generation of Lentiviral Particles Containing shRNAs. MISSION pLKO.1-puro empty vector control plasmid DNA (Sigma-Aldrich) was used for this subcloning. We designed mouse ADAM9-shRNA as listed below and subcloned them into the empty vector following the manufacturer's protocols. The following oligonucleotide sequences were used for this subcloning: 5′-CCGGCCTGAATTATGACTGTGACATCTCGAGATGTCACAGTCATAATTCAGGTTTTTG-3′ and 5′-AATTCAAAAACCTGAATTATGACTGTGACATCTCGAGATGTCACAGTCATAATTCAGG-3′. Sequences of cloned vectors were verified (Genewiz). MISSION pLKO.1-puro nonmammalian shRNA Control Plasmid DNA (Sigma-Aldrich) was used for control shRNA. Those vectors were transfected to 40% confluent HEK-293T cells by polyethyleneimine "Max" (Polysciences, Inc.) according to the manufacturer's protocol. Culture media with shRNA-contained lentiviral particles were collected by using Lenti-X Concentrator (Takara Bio) on day 3 and day 4.

Transfection of shRNA to Murine Primary T Cells. Naïve CD4$^+$ T cells from murine spleens were cultured under Th17 cell conditions. On day 1 of culture, ADAM9-shRNA or control-shRNA-containing lentiviral particles were added to media with polybrene infection/transfection reagent (Sigma-Aldrich). One day after infection, puromycin was added to the media. Cultured cells were harvested and analyzed on day 4 of culture.

CRISPR editing human primary CD4$^+$ T cells. Guide RNAs for CRISPR editing were designed using Benchling, and chemically modified synthetic guide RNAs (sgRNAs) were synthesized by Synthego. The following sequences were used for CRISPR editing: 5′-TTGTCATTATCGGGGCTATG-3′, 5′-CATTATCGGGGCTATGTGGA-3′, and 5′-AGTAGCTGAGTCATGCTGGG-3′ for pooled human ADAM9 targeting sgRNAs. Nontargeting sgRNA was used as a negative control. To prepare ribonucleoprotein complexes, a total of 50 pmols of pooled three targeting sgRNAs or nontarget sgRNA were mixed with 20 pmols of Cas9 2NLS nuclease (*Streptococcus pyogenes*) (New England Biolabs) and incubated at room temperature for 10 min. For ADAM9 deletion in human primary T cells, human naïve CD4$^+$ T cells were isolated from SLE patients and were cultured in Th17-polarizing conditions. Cells were harvested 2 d after starting culture, and pooled ADAM9 targeting or nontargeting sgRNAs were transfected using the Amaxa human T Cell Nucleofector Kit with the T-020 program. After transfection, cells were transferred into the Th17-polarizing culture media and were incubated for another 5 d.

In vitro cleavage assay for LAP by recombinant ADAM9. A total of 50 ng of human latent TGF-β1 was incubated with human recombinant ADAM9 protein (R&D Systems) for 16 h in 20 μL of tris(hydroxymethyl)aminomethane (Tris) assay buffer (50 mM Tris·HCl, pH 7.5, 150 mM NaCl, and 10 mM CaCl2) at 37 °C.

Cleavage of LAP by murine primary T cell cultured in vitro. Purified naive murine CD4$^+$ T cells were cultured under Th17 or Treg conditions. After 48 h of incubation, 0.5 million cells were incubated under Th17 or Treg conditions with latent TGF-β1 (1.0 ng/mL for Th17, 3.0 ng/mL for Treg) for an additional 16 h. The levels of LAP in the culture supernatants were determined by ELISA.

Luciferase Assay. Mouse *adam9* promoter luciferase reporter construct (pGL3_madam9_vector) was purchased from GenScript. Site-directed mutagenesis at the −193/−189 CRE site (CGTCA) within pGL3_madam9_vector was performed by using the Q5 Site-Directed Mutagenesis Kit (New England Biolabs) with the following primers: 5′-GCCTCTGGCCGCGGGATC-3′ and 5′-TAGGGAAAATACAGTCTGGCCAACCC-3′. All sequences were verified (Genewiz). Luciferase reporter plasmid was transfected using the Amaxa Mouse T Cell Nucleofector Kit with the X-001 program on day 2 of culture. Each reporter experiment included 200 ng of renilla luciferase construct as an internal control. Luciferase activity was quantified using the Promega Dual Luciferase Assay System (Promega) on day 3 of culture according to the manufacturer's instructions.

Chromatin Immunoprecipitation Assays. Freshly isolated naïve CD4$^+$ T cells from B6.ICER/CREM$^{-/-}$ mice were cultured in Th17-polarizing conditions for 3 d. N′-FLAG-tagged ICERγ overexpressing vectors (35) were transfected as described above on day 1. Harvested cells were lysed, and ChIP assay was performed using the MAGnify Chromatin Immunoprecipitation System (Thermo Fisher Scientific). Anti-FLAG antibody produced in rabbit (Sigma-Aldrich) was used for immunoprecipitation. The following primer pairs were used: 5′-TTCCCTACGTCAGCCTCTG-3′ and 5′-TTCGGTCATCCTTGCAACC-3′ for the *Adam9* promoter region-containing CRE site, 5′- CTGGGAGATGGAACTTTTGC-3′and 5′-GGGATCCCTGTGGACCTACT-3′ for the *Adam9* intron1-containing CRE site, and 5′-CTTTTCCTCCTGGTTGTTGC-3′and 5′-CGCTTGGCTAGAGGTACCAG-3′ for the other gene *(Tm2d2)* intron3-containing CRE site, which is located beside the *Adam9* gene. The ChIP assay for detecting the accumulation of RORγt was performed using naïve CD4$^+$ T cells from B6 mice and RORγt monoclonal antibody (Thermo Fisher Scientific, clone: AFKJS-9). All other conditions were identical to those described for the detection of ICER accumulation.

EAE. On day 0, 8 wk old mice were immunized subcutaneously with 200 μg MOG_{35-55} peptide (AnaSpec) emulsified in the complete Freund's adjuvant containing 4 mg/mL *Mycobacterium tuberculosis* extract (H37Ra) (Chondrex). On days 0 and 2, 200 ng pertussis toxin (List Labs, Campbell) per mouse was given by intraperitoneal injection. Mice were monitored and weighed daily until day 28 of the experiment. The following clinical scores were used: 1, limp tail; 2, hind-limb paresis; 3, hind-limb paralysis; 4, tetraplegia; and 5, moribund (35).

Adoptive Transfer EAE. Naive CD4$^+$ T cells from 2D2 mice or *Adam9*$^{-/-}$.2D2 mice were cultured under Th17-polarizing conditions. Cultured cells were harvested on day 3 of culture. Two million cells were suspended in 150 μL of PBS (pH 7.4) and intravenously delivered into each 8 wk old Rag1-deficient mouse using retro-orbital sinus injection. Pertussis toxin (300 ng per mouse) was intraperitoneally injected later on the day of transfer and 2 d. Mice were monitored and weighed as previously described.

Histological Staining and Analysis. Sections from 10% formalin-fixed spinal cords were stained with hematoxylin and eosin. Spinal cord sections were scored by an investigator blinded to the experimental group as follows: 0, no infiltration (<50 cells); 1, mild infiltration of nerve or nerve sheath (50 to 100 cells); 2, moderate infiltration (100 to 150 cells); 3, severe infiltration (150 to 200 cells); and 4, massive infiltration (>200 cells).

Statistical Analyses. Comparisons between two different groups were done by unpaired two-tailed Student's *t*-test. Comparisons between two related groups were done by paired *t*-test. Comparisons between more than two groups were done by one-way ANOVA (with Tukey's multiple-comparisons posttests). For the EAE experiments, clinical scores in each treatment group were compared by two-way ANOVA. Statistical analyses were performed with GraphPad Prism 7.0 software (GraphPad Software). P values < 0.05 were considered significant.

Data Availability. All study data are included in the article and/or supporting information.

ACKNOWLEDGMENTS. This work was supported by NIH grant R37 AI49954 (to G.C.T.) and the Gilead Sciences Research Scholars Program in Rheumatology (to N.Y.).

1. G. C. Tsokos, Systemic lupus erythematosus. *N. Engl. J. Med.* **365**, 2110–2121 (2011).
2. T. Koga, K. Ichinose, A. Kawakami, G. C. Tsokos, The role of IL-17 in systemic lupus erythematosus and its potential as a therapeutic target. *Expert Rev. Clin. Immunol.* **15**, 629–637 (2019).
3. W. Ouyang, J. K. Kolls, Y. Zheng, The biological functions of T helper 17 cell effector cytokines in inflammation. *Immunity* **28**, 454–467 (2008).
4. P. R. Burkett, G. Meyer zu Horste, V. K. Kuchroo, Pouring fuel on the fire: Th17 cells, the environment, and autoimmunity. *J. Clin. Invest.* **125**, 2211–2219 (2015).
5. C. K. Wong *et al*., Hyperproduction of IL-23 and IL-17 in patients with systemic lupus erythematosus: Implications for Th17-mediated inflammation in auto-immunity. *Clin. Immunol.* **127**, 385–393 (2008).
6. D. Y. Chen *et al*., The potential role of Th17 cells and Th17-related cytokines in the pathogenesis of lupus nephritis. *Lupus* **21**, 1385–1396 (2012).
7. E. Bettelli *et al*., Reciprocal developmental pathways for the generation of pathogenic effector TH17 and regulatory T cells. *Nature* **441**, 235–238 (2006).
8. D. Young, N. Das, A. Anowai, A. Dufour, Matrix metalloproteases as influencers of the cells' social media. *Int. J. Mol. Sci.* **20**, 3847 (2019).
9. B. N. Lambrecht, M. Vanderkerken, H. Hammad, The emerging role of ADAM metalloproteinases in immunity. *Nat. Rev. Immunol.* **18**, 745–758 (2018).
10. S. Riethmueller *et al*., Cleavage site localization differentially controls interleukin-6 receptor proteolysis by ADAM10 and ADAM17. *Sci. Rep.* **6**, 25550 (2016).
11. A. Sharabi *et al*., PP2A enables IL-2 signaling by preserving IL-2Rβ chain expression during Treg development. *JCI Insight* **5**, e126294 (2019).
12. J. J. Orme *et al*., Heightened cleavage of Axl receptor tyrosine kinase by ADAM metalloproteases may contribute to disease pathogenesis in SLE. *Clin. Immunol.* **169**, 58–68 (2016).
13. F. S. Hoffmann *et al*., The immunoregulator soluble TACI is released by ADAM10 and reflects B cell activation in autoimmunity. *J. Immunol.* **194**, 542–552 (2015).
14. B. Jones, A. E. Koch, S. Ahmed, Pathological role of fractalkine/CX3CL1 in rheumatic diseases: A unique chemokine with multiple functions. *Front. Immunol.* **2**, 82 (2012).
15. G. Weskamp, J. Krätzschmar, M. S. Reid, C. P. Blobel, MDC9, a widely expressed cellular disintegrin containing cytoplasmic SH3 ligand domains. *J. Cell Biol.* **132**, 717–726 (1996).
16. D. A. Parry *et al*., Loss of the metalloprotease ADAM9 leads to cone-rod dystrophy in humans and retinal degeneration in mice. *Am. J. Hum. Genet.* **84**, 683–691 (2009).
17. V. Guaiquil *et al*., ADAM9 is involved in pathological retinal neovascularization. *Mol. Cell. Biol.* **29**, 2694–2703 (2009).
18. R. Grützmann *et al*., ADAM9 expression in pancreatic cancer is associated with tumour type and is a prognostic factor in ductal adenocarcinoma. *Br. J. Cancer* **90**, 1053–1058 (2004).
19. F. R. Fritzsche *et al*., ADAM9 is highly expressed in renal cell cancer and is associated with tumour progression. *BMC Cancer* **8**, 179 (2008).
20. L. Peduto, V. E. Reuter, D. R. Shaffer, H. I. Scher, C. P. Blobel, Critical function for ADAM9 in mouse prostate cancer. *Cancer Res.* **65**, 9312–9319 (2005).
21. K. Namba *et al*., Involvement of ADAM9 in multinucleated giant cell formation of blood monocytes. *Cell. Immunol.* **213**, 104–113 (2001).
22. Y. Izumi *et al*., A metalloprotease-disintegrin, MDC9/meltrin-gamma/ADAM9 and PKCdelta are involved in TPA-induced ectodomain shedding of membrane-anchored heparin-binding EGF-like growth factor. *EMBO J.* **17**, 7260–7272 (1998).
23. R. Roychaudhuri *et al*., ADAM9 is a novel product of polymorphonuclear neutrophils: Regulation of expression and contributions to extracellular matrix protein degradation during acute lung injury. *J. Immunol.* **193**, 2469–2482 (2014).
24. T. S. Heng, M. W. Painter; Immunological Genome Project Consortium, The immunological genome project: Networks of gene expression in immune cells. *Nat. Immunol.* **9**, 1091–1094 (2008).
25. J. P. Annes, J. S. Munger, D. B. Rifkin, Making sense of latent TGFbeta activation. *J. Cell Sci.* **116**, 217–224 (2003).
26. M. A. Travis, D. Sheppard, TGF-β activation and function in immunity. *Annu. Rev. Immunol.* **32**, 51–82 (2014).
27. R. M. Lyons, J. Keski-Oja, H. L. Moses, Proteolytic activation of latent transforming growth factor-beta from fibroblast-conditioned medium. *J. Cell Biol.* **106**, 1659–1665 (1988).
28. L. C. Bridges, R. D. Bowditch, ADAM-integrin interactions: Potential integrin regulated ectodomain shedding activity. *Curr. Pharm. Des.* **11**, 837–847 (2005).
29. G. J. Thomas, I. R. Hart, P. M. Speight, J. F. Marshall, Binding of TGF-beta1 latency-associated peptide (LAP) to alpha(v)beta6 integrin modulates behaviour of squamous carcinoma cells. *Br. J. Cancer* **87**, 859–867 (2002).
30. R. M. Mahimkar, O. Visaya, A. S. Pollock, D. H. Lovett, The disintegrin domain of ADAM9: A ligand for multiple beta1 renal integrins. *Biochem. J.* **385**, 461–468 (2005).
31. M. J. McGeachy *et al*., TGF-beta and IL-6 drive the production of IL-17 and IL-10 by T cells and restrain T(H)-17 cell-mediated pathology. *Nat. Immunol.* **8**, 1390–1397 (2007).
32. S. Abdollah *et al*., TbetaRI phosphorylation of Smad2 on Ser465 and Ser467 is required for Smad2-Smad4 complex formation and signaling. *J. Biol. Chem.* **272**, 27678–27685 (1997).
33. X. Liu *et al*., Transforming growth factor beta-induced phosphorylation of Smad3 is required for growth inhibition and transcriptional induction in epithelial cells. *Proc. Natl. Acad. Sci. U.S.A.* **94**, 10669–10674 (1997).
34. G. J. Martinez *et al*., Smad2 positively regulates the generation of Th17 cells. *J. Biol. Chem.* **285**, 29039–29043 (2010).
35. N. Yoshida *et al*., ICER is requisite for Th17 differentiation. *Nat. Commun.* **7**, 12993 (2016).
36. A. X. Zhou, A. El Hed, F. Mercer, L. Kozhaya, D. Unutmaz, The metalloprotease ADAM12 regulates the effector function of human Th17 cells. *PLoS One* **8**, e81146 (2013).
37. M. A. Link *et al*., The role of ADAM17 in the T-cell response against bacterial pathogens. *PLoS One* **12**, e0184320 (2017).
38. I. Gutcher *et al*., Autocrine transforming growth factor-β1 promotes in vivo Th17 cell differentiation. *Immunity* **34**, 396–408 (2011).
39. D. Zhang *et al*., High glucose intake exacerbates autoimmunity through reactive-oxygen-species-mediated TGF-β cytokine activation. *Immunity* **51**, 671–681.e5 (2019).
40. T. Rauen, C. M. Hedrich, Y. T. Juang, K. Tenbrock, G. C. Tsokos, cAMP-responsive element modulator (CREM)α protein induces interleukin 17A expression and mediates epigenetic alterations at the interleukin-17A gene locus in patients with systemic lupus erythematosus. *J. Biol. Chem.* **286**, 43437–43446 (2011).
41. C. M. Hedrich *et al*., cAMP response element modulator α controls IL2 and IL17A expression during CD4 lineage commitment and subset distribution in lupus. *Proc. Natl. Acad. Sci. U.S.A.* **109**, 16606–16611 (2012).
42. T. Maretzky *et al*., Characterization of the catalytic properties of the membrane-anchored metalloproteinase ADAM9 in cell-based assays. *Biochem. J.* **474**, 1467–1479 (2017).
43. E. C. Baechler *et al*., Interferon-inducible gene expression signature in peripheral blood cells of patients with severe lupus. *Proc. Natl. Acad. Sci. U.S.A.* **100**, 2610–2615 (2003).
44. S. Stanley *et al*., Comprehensive aptamer-based screening identifies a spectrum of urinary biomarkers of lupus nephritis across ethnicities. *Nat. Commun.* **11**, 2197 (2020).
45. M. C. Hochberg, Updating the American College of Rheumatology revised criteria for the classification of systemic lupus erythematosus. *Arthritis Rheum.* **40**, 1725 (1997).
46. C. Bombardier, D. D. Gladman, M. B. Urowitz, D. Caron, C. H. Chang; The Committee on Prognosis Studies in SLE, Derivation of the SLEDAI. A disease activity index for lupus patients. *Arthritis Rheum.* **35**, 630–640 (1992).
47. J. A. Blendy, K. H. Kaestner, G. F. Weinbauer, E. Nieschlag, G. Schütz, Severe impairment of spermatogenesis in mice lacking the CREM gene. *Nature* **380**, 162–165 (1996).
48. G. Weskamp *et al*., Mice lacking the metalloprotease-disintegrin MDC9 (ADAM9) have no evident major abnormalities during development or adult life. *Mol. Cell. Biol.* **22**, 1537–1544 (2002).
49. H. X. Nguyen, K. D. Beck, A. J. Anderson, Quantitative assessment of immune cells in the injured spinal cord tissue by flow cytometry: A novel use for a cell purification method. *J. Vis. Exp.* 2698 (2011).
50. V. A. Gerriets *et al*., Metabolic programming and PDHK1 control CD4+ T cell subsets and inflammation. *J. Clin. Invest.* **125**, 194–207 (2015).